New electromechanical substrate abnormalities in high-risk patients with Brugada syndrome

Carlo Pappone, MD, PhD,* Valerio Mecarocci, MD,* Francesco Manguso, MD, PhD,* Giuseppe Ciconte, MD,* Gabriele Vicedomini, MD,* Francesco Sturla, PhD,† Emiliano Votta, PhD,‡ Beniamino Mazza, BEng,* Paolo Pozzi, BEng,* Valeria Borrelli, PhD,* Luigi Anastasia, PhD,§ Emanuele Micaglio, MD,* Emanuela Locati, MD,* Michelle M. Monasky, PhD,* Massimo Lombardi, MD,‖ Zarko Calovic, MD,* Vincenzo Santinelli, MD*

*From the *Arrhythmology Department, IRCCS Policlinico San Donato, San Donato Milanese, Italy, †Computer Simulation Laboratory, IRCCS Policlinico San Donato, San Donato Milanese, Italy, ‡Department of Electronics, Information and Bioengineering, Politecnico di Milano, Milan, Italy, §Department of Biomedical Sciences for Health, University of Milan, Milan, Italy, and ‖Department of Cardiovascular Imaging, Policlinico San Donato, San Donato Milanese, Italy.*

BACKGROUND The relationship between the typical electrocardiographic pattern and electromechanical abnormalities has never been systematically explored in Brugada syndrome (BrS).

OBJECTIVES The aims of this study were to characterize the electromechanical substrate in patients with BrS and to evaluate the relationship between electrical and mechanical abnormalities.

METHODS We enrolled 50 consecutive high-risk patients with BrS (mean age 42 ± 7.2 years), with implantable cardioverter-defibrillator implantation for primary or secondary prevention of ventricular tachyarrhythmias (ventricular tachycardia/ventricular fibrillation [VT/VF]), undergoing substrate mapping and ablation. Patients underwent 3-dimensional (3D) echocardiography with 3D wall motion/deformation quantification and electroanatomic mapping before and after ajmaline administration (1 mg/kg in 5 minutes); 3D mechanical changes were compared with 50 age- and sex-matched controls. The effect of substrate ablation on electromechanical abnormalities was also assessed.

RESULTS In all patients, ajmaline administration induced Brugada type 1 pattern, with a significant increase in the electrical substrate ($P < .001$), particularly in patients with previous spontaneous VT/VF ($P = .007$). Induction of Brugada pattern was associated with lowering of right ventricular (RV) ejection fraction ($P < .001$) and worsening of 3D RV mechanical function ($P < .001$), particularly in the anterior free wall of the RV outflow tract, without changes in controls. RV electrical and mechanical abnormalities were highly correlated ($r = 0.728$, $P < .001$). By multivariate analysis, only the area of RV dysfunction was an independent predictor of spontaneous VT/VF (odds ratio 1.480; 95% confidence interval 1.159–1.889; $P = .002$). Substrate ablation abolished both BrS-electrocardiographic pattern and mechanical abnormalities, despite ajmaline rechallenge.

CONCLUSION BrS is an electromechanical disease affecting the RV. The typical BrS pattern reflects an extensive RV arrhythmic substrate, driving consistent RV mechanical abnormalities. Substrate ablation abolished both Brugada pattern and mechanical abnormalities.

KEYWORDS Arrhythmic substrate; Brugada syndrome; Echocardiography; Mapping; Right ventricular function; Sudden cardiac death

(Heart Rhythm 2020;17:637–645)

Introduction

Over the years since the syndrome was first described in 1992, the exact mechanism of the typical electrocardiographic (ECG) pattern is still unknown, remaining elusive and not well explained.[1] It is well documented that before ventricular fibrillation (VF), type 1 ECG pattern with ST-segment elevation becomes more prominent and is often accompanied by shortly coupled premature ventricular complexes that initiate fatal arrhythmias.[2] Besides, commonly there is a substantial day-to-day variability in the ECG pattern characteristics, even in patients experiencing cardiac arrest, in whom it can even disappear temporarily. Therefore, ajmaline provocation has been widely used to unmask the hallmark of the syndrome.[1] In the last years, 3-dimensional (3D) cardiac imaging modality has gained more attention and interest in patients with Brugada syndrome (BrS), where

This study was supported by the Arrhythmology Department of IRCCS Policlinico San Donato, San Donato Milanese, Milan, Italy. **Address reprint requests and correspondence:** Dr Carlo Pappone, Department of Arrhythmology, IRCCS Policlinico San Donato, Piazza E Malan, 20097 San Donato Milanese, Italy. E-mail address: carlo.pappone@af-ablation.org.

1547-5271/

https://doi.org/10.1016/j.hrthm.2019.11.019

extensive arrhythmic substrates have been identified, particularly in the right ventricular outflow tract (RVOT) as the origin for ventricular tachycardia (VT)/VF.[3–7] In addition, there is considerable growing interest and accumulating evidence for the presence of right ventricular (RV) mechanical changes, with a reported prevalence, which varied widely across the published studies.[8–21] We hypothesized that the RV mechanical changes correlate with electrical substrate abnormalities and the typical BrS-ECG pattern. Therefore, the aims of this study were to systematically characterize the mechanical and electrical changes in a series of consecutive high-risk patients with BrS in the presence of a stable type 1 Brugada pattern and to explore the relationship between electrical and mechanical changes by using a multimodality 3D imaging protocol.

Methods

Study population

This study includes a series of 50 consecutive patients diagnosed to be affected by BrS, with either spontaneous or ajmaline-induced type 1 Brugada ECG pattern, with previous implantable cardioverter-defibrillator (ICD) implantation, participating in an investigational prospective registry study (Epicardial ablation in Brugada syndrome: an extension study of 500 Brs patients; clinicaltrials.gov identifier: NCT03106701). The investigational protocol is reported in the Supplemental Appendix.

3D imaging study protocol

Transthoracic 2D and 3D echocardiography was performed to evaluate the RV and left ventricular (LV) global function with 3D regional wall motion parameters according to the recommendations of the American Society of Echocardiography and the European Association of Cardiovascular Imaging.[22] Details on 3D echocardiography and motion/deformation parameters are reported in the Supplemental Appendix (Supplemental Figures 1–6).

Substrate mapping and ablation

Electroanatomic maps were obtained during stable sinus rhythm using the CARTO 3 system (Biosense Webster, Diamond Bar, CA) with incorporated area calculation software to accurately define the areas of low-voltage and delayed fragmented abnormal electrograms, as previously reported in detail.[4–6] Details of substrate mapping are reported in the Supplemental Appendix. Radiofrequency (RF) ablation was delivered during sinus rhythm with an externally irrigated 3.5-mm-tip ablation catheter (ThermoCool SF, NaviStar, Biosense Webster), as previously reported.[4–6] Briefly, a 35–42 W power control mode was used with an irrigation rate of 17 mL/min during ablation. RF energy was applied by a dragging technique up to 10-second duration per point, and RF applications were repeated up to complete elimination of all long-duration and delayed electrograms. When ajmaline challenge proved both fragmented activity abolition and BrS-ECG pattern elimination, VT/VF inducibility was reassessed. Further details on substrate ablation are given in the Supplemental Appendix. Three months after ablation, ECG and 3D echocardiography were systematically repeated before and after ajmaline administration to ensure the normalization of both BrS-ECG pattern and mechanical abnormalities.

Statistical analysis

Categorical variables were compared using the χ^2 test. Continuous variables were reported as mean values ± SDs or median values with 25th and 75th percentiles depending on their distribution. Continuous variables with normal distribution were compared using paired and unpaired *t* tests. In the case of nonnormality distribution, data were compared using the Mann-Whitney *U* test. Multivariate binary logistic regression was used to evaluate the relationship between the presence of spontaneous VT/VF (no/yes = 0/1) as the dependent variables and possible noninvasive predictors as the independent variables. Details on multivariate analysis methodology are given in the Supplemental Appendix. Intra- and interobserver reproducibility was analyzed using both bivariate 2-tailed Pearson correlation test and Bland-Altman analysis (with 95% agreement limits). Values of $P < .05$ (2-tailed) were taken as statistically significant. IBM SPSS Statistics for Windows version 25.0 (IBM Corporation, Armonk, NY) was used for the statistical analysis.

Results

Baseline data

A total of 50 eligible high-risk patients with BrS were included in the study population. The baseline characteristics of the study population are summarized in Supplemental Table 1. Among enrolled patients, spontaneous type 1 BrS ECG pattern was present in 20 patients (40%). An ICD was implanted for secondary prevention in 35 of 50 patients (70%) because of sustained episodes of VT/VF; among them, 16 patients had evidence of spontaneous type 1 ECG pattern. Primary prevention ICD therapy included 15 patients with a family history of sudden cardiac death, experiencing syncope, dizziness or palpitations of suspected arrhythmic origin, and/or frequent episodes of nonsustained ventricular tachyarrhythmias occasionally documented on ECG recordings. During electrophysiology study, these 15 patients had inducible polymorphic VT rapidly degenerating into VF requiring multiple DC shocks and life support for termination; after ICD implantation, they experienced occasional episodes of self-terminating VT/VF requiring ICD therapy in 3 patients; 4 presented with spontaneous type 1 ECG pattern. Although patients receiving ICD for secondary prevention were younger than those in primary prevention (mean age 40 ± 7 years vs 46 ± 7 years; $P = .005$), sex, family history of sudden cardiac death, type 1 BrS-ECG pattern, and genetic testing were similar in both groups. Appropriate ICD therapy occurred over a median follow-up period of 21 months in 19 of 50 patients (38%), of whom 16 in secondary prevention.

Genetic tests were obtained in all patients, and 9 of them were positive for a mutation in the *SCN5A* gene; 6 genotype-positive patients had type 1 ECG pattern (Supplemental Table 2).

ECG parameters

Heart rate, PR interval, QRS interval, and corrected QT interval increased after ajmaline in both patients with BrS and healthy controls without between-group differences (Supplemental Table 3). After ajmaline, ECG changes were similar in patients with and without spontaneous type 1 ECG pattern (Supplemental Table 4). Before and after ajmaline administration, neither patients with BrS nor controls had conduction disturbances including atrioventricular or left or right bundle branch block.

Preablation echocardiography

Under baseline conditions, although the RV ejection fraction was within the normal range, it was significantly lower in the subgroup of patients with spontaneous type 1 BrS ECG pattern (Supplemental Table 3). After ajmaline, patients with BrS showed larger 3D RV end-diastolic volume and lower 3D RV ejection fraction with respect to controls. Noteworthy, LV echocardiographic parameters at baseline and after ajmaline were similar in the whole study population (Supplemental Table 3). Between patients receiving ICD for secondary and primary prevention, no differences were

Table 1 Right ventricular mechanical changes in 50 patients with BrS and in 50 controls before and after ajmaline administration

	Patients with BrS (n = 50)			Controls (n = 50)				
Variable	Baseline	Ajmaline	P^*	Baseline	Ajmaline	P^*	$P^\dagger$	$P^\ddagger$
Normal displacement								
Anterior								
Absolute values (mm)	−3.31 ± 1.71	0.19 ± 1.81	<.001	−3.03 ± 1.59	−3.24 ± 1.91	.39	.40	<.001
Time to peak (ms)	40 ± 6	41 ± 7	.246	39 ± 7	40 ± 7	.06	.61	.630
Lateral								
Absolute values (mm)	−9.37 ± 1.81	−8.49 ± 1.57	.007	−9.49 ± 1.76	−9.31 ± 1.58	.54	.74	.010
Time to peak (ms)	39 ± 6	41 ± 7	<.001	39 ± 6	39 ± 7	.81	.80	.060
RVOT								
Absolute values (mm)	−6.61 ± 2.24	−4.70 ± 2.18	<.001	−5.98 ± 1.81	−5.55 ± 1.51	.14	.13	.030
Time to peak (ms)	42 ± 6	44 ± 7	.016	40 ± 6	40 ± 6	.14	.07	.010
Inferior								
Absolute values (mm)	−6.39 ± 1.61	−6.13 ± 1.48	.285	−5.97 ± 1.35	−5.68 ± 1.18	.05	.16	.100
Time to peak (ms)	40 ± 5	41 ± 6	.003	38 ± 5	38 ± 6	.64	.11	.006
Areal strain								
Anterior								
Absolute values (%)	−39.18 ± 8.10	−26.29 ± 7.05	<.001	−40.33 ± 7.21	−37.53 ± 5.66	.016	.45	<.001
Time to peak (ms)	39 ± 5	43 ± 8	<.001	39 ± 7	39 ± 7	.682	.84	.022
Lateral								
Absolute values (%)	−47.52 ± 6.47	−40.80 ± 6.04	<.001	−45.96 ± 5.76	−43.97 ± 6.89	.056	.20	.016
Time to peak (ms)	39 ± 6	41 ± 7	.001	37 ± 6	38 ± 7	.295	.21	.025
RVOT								
Absolute values (%)	−26.73 ± 7.56	−16.75 ± 7.65	<.001	−21.22 ± 7.06	−21.79 ± 7.59	.562	<.001	.001
Time to peak (ms)	41 ± 6	45 ± 9	<.001	41 ± 7	40 ± 7	.347	.78	.003
Inferior								
Absolute values (%)	−42.32 ± 6.79	−40.39 ± 5.89	.075	−43.92 ± 5.40	−41.87 ± 6.36	.013	.20	.230
Time to peak (ms)	38 ± 6	41 ± 6	<.001	38 ± 7	39 ± 7	.034	.58	.054
Minimum principal strain								
Anterior								
Absolute values (%)	−32.52 ± 7.19	−24.01 ± 5.71	<.001	−33.54 ± 5.74	−33.27 ± 5.96	.110	.43	<.001
Time to peak (ms)	41 ± 6	43 ± 8	.002	39 ± 6	40 ± 7	.258	.07	.016
Lateral								
Absolute values (%)	−39.62 ± 4.46	−34.22 ± 5.70	<.001	−38.00 ± 6.05	−36.89 ± 6.92	.187	.13	.037
Time to peak (ms)	39 ± 5	41 ± 7	.005	37 ± 6	38 ± 6	.110	.07	.014
RVOT								
Absolute values (%)	−23.70 ± 3.27	−17.12 ± 4.57	<.001	−21.50 ± 5.25	−21.16 ± 7.20	.187	.013	.001
Time to peak (ms)	41 ± 6	44 ± 7	<.001	40 ± 6	40 ± 7	.201	.26	.012
Inferior								
Absolute values (%)	−33.39 ± 4.86	−32.64 ± 4.86	.336	−35.35 ± 4.72	−34.66 ± 5.55	.205	.04	.056
Time to peak (ms)	39 ± 5	41 ± 7	<.001	37 ± 6	38 ± 6	.219	.22	.010

BrS = Brugada syndrome; RVOT = right ventricular outflow tract.

*Baseline vs ajmaline.

†Between baseline values of the 2 groups.

‡Between ajmaline values of the 2 groups.

observed at baseline and after ajmaline in all 3D RV and LV echocardiographic parameters.

Table 1 presents the 3D motion/deformation changes at baseline and after ajmaline. In the control group, ajmaline did not induce any change in such parameters, while in patients with BrS, a significant worsening of normal displacement, areal strain, and minimum principal strain occurred after ajmaline in different regions of the RV (Table 1; Supplemental Figure 5). Specifically, the entity of areal strain significantly decreased after ajmaline in the RV anterior, lateral, and RVOT free wall, and this reduction was associated with a significant delay of activation (time to peak) (Table 1). Before RF ablation, the extent of the RV dysfunction area induced by ajmaline was significantly larger in patients with BrS than in controls ($P < .001$) (Table 2), with the anterior RV free wall being the largest affected area. The total area of RV dysfunction was larger in patients with type 1 ECG than in the subgroup of patients with no type 1 ECG (38.52 ± 11.64 cm^2 vs 31.04 ± 5.89 cm^2; $P = .004$). Similarly, larger areas of RV dysfunction were found in the secondary prevention group than in the primary prevention group (38.03 ± 6.07 cm^2 vs 26.69 ± 8.99 cm^2; $P < .001$). Figures 1 and 2 show an example of ajmaline-induced RVOT contractility reduction in 2 patients with and without spontaneous type 1 BrS-ECG pattern.

Substrate mapping and ablation

The median procedure and RF application times were 158 minutes (interquartile range [IQR] 138–184 minutes; range 98–255 minutes) and 17 minutes (IQR 15–19.7 minutes; range 5–30 minutes), respectively. RF energy was applied before and after ajmaline administration, with a median duration of 7 seconds for each application. Areas of delayed fractionated electrograms were recorded exclusively in RV epicardial maps. Overall, before ajmaline such areas were highly variable for extension and distribution, ranging from 0 to a maximum of 23.2 cm^2. Patients with spontaneous type 1 BrS-ECG pattern showed larger substrate areas than did patients with concealed ECG pattern before and after ajmaline administration (Supplemental Table 4). Patients with ICD for secondary and primary prevention exhibited similar substrate sizes at baseline (8.28 ± 6.80 cm^2 vs 5.37 ± 5.02 cm^2, respectively; $P = .101$), while larger areas were found after ajmaline in the secondary prevention group (21.92 ± 5.28 cm^2 vs 16.96 ± 6.79 cm^2, respectively; $P = .007$). Overall, the duration of abnormal electrograms also increased after ajmaline from a median of 226 ms (IQR 154–305 ms; range 69–327 ms) to 315 ms (IQR 267–436 ms; range 219–482 ms) ($P < .001$), while bipolar voltage decreased from a median of 2.0 mV (IQR 1.60–3.11 mV) to 1.37 mV (IQR 1.19–1.61 mV) after ajmaline ($P < .001$). Patients with spontaneous type 1 BrS-ECG pattern showed more prolonged abnormal potentials than did patients with concealed ECG pattern both before and after ajmaline administration ($P < .001$). In particular, the potential duration increased from a median of 306 ms (IQR 298–317 ms; range 215–327 ms) to 439 ms (IQR 431–480 ms; range 307–482 ms) in the type 1 ECG pattern group and from 168 ms (IQR 140–226 ms; range 69–312 ms) to 278 ms (IQR 239–315 ms; range 219–392 ms) in no type 1 ECG pattern group. No differences in potential duration both before and after ajmaline administration were found between patients receiving ICD for primary and secondary prevention. Abnormal electrograms were not found at the endocardial site of the same area of the RVOT. After ablation, small low-voltage areas (median 1 cm^2) without scar tissue were detected inside the substrate area (Supplemental Figures 7 and 8). RF ablation began on areas with the widest fragmented activity, which, during ablation, disappeared without a significant change in voltage amplitude after RF was turned off. Twenty patients after ajmaline rechallenge showed the reappearance of suspicious coved ECG pattern, requiring further RF ablation to eliminate any residual fragmented electrical activity leading to ECG pattern normalization. Epicardial ablation resulted in the normalization of Brugada ECG pattern in all patients. Immediately after, there was a typical flat ST-segment elevation progressively becoming ascendant in leads V_1 and V_2, which was not further modified by ajmaline. After substrate ablation, all patients became noninducible for VT/VF despite ajmaline provocation.

Correlation between abnormal mechanical area and electrical substrate area

We observed a significant correlation between the RV 3D dysfunction area and the 3D electrical substrate size after

Table 2 Pre- and post-RFA ajmaline-induced RV dysfunction area in 50 patients with BrS

	Normal displacement area (cm^2)					
	Patients with BrS (n = 50					
Variable	Pre-RFA	Post-RFA	Controls (n = 50)	P*	$P^{\dagger}$	$P^{\ddagger}$
Total	34.03 ± 9.32	12.70 ± 9.99	12.08 ± 10.01	<.001	.756	<.001
Anterior	15.20 ± 4.35	3.35 ± 3.90	3.24 ± 3.98	<.001	.893	<.001
Lateral	11.60 ± 5.65	6.95 ± 5.92	6.75 ± 6.13	<.001	.871	<.001
RVOT	7.24 ± 3.23	3.62 ± 3.31	2.87 ± 3.28	<.001	.260	<.001

BrS = Brugada syndrome; RFA = RF ablation; RV = right ventricular; RVOT = right ventricular outflow tract.

*Pre-RFA vs controls.

†Post-RFA vs controls.

‡Pre-RFA vs post-RFA.

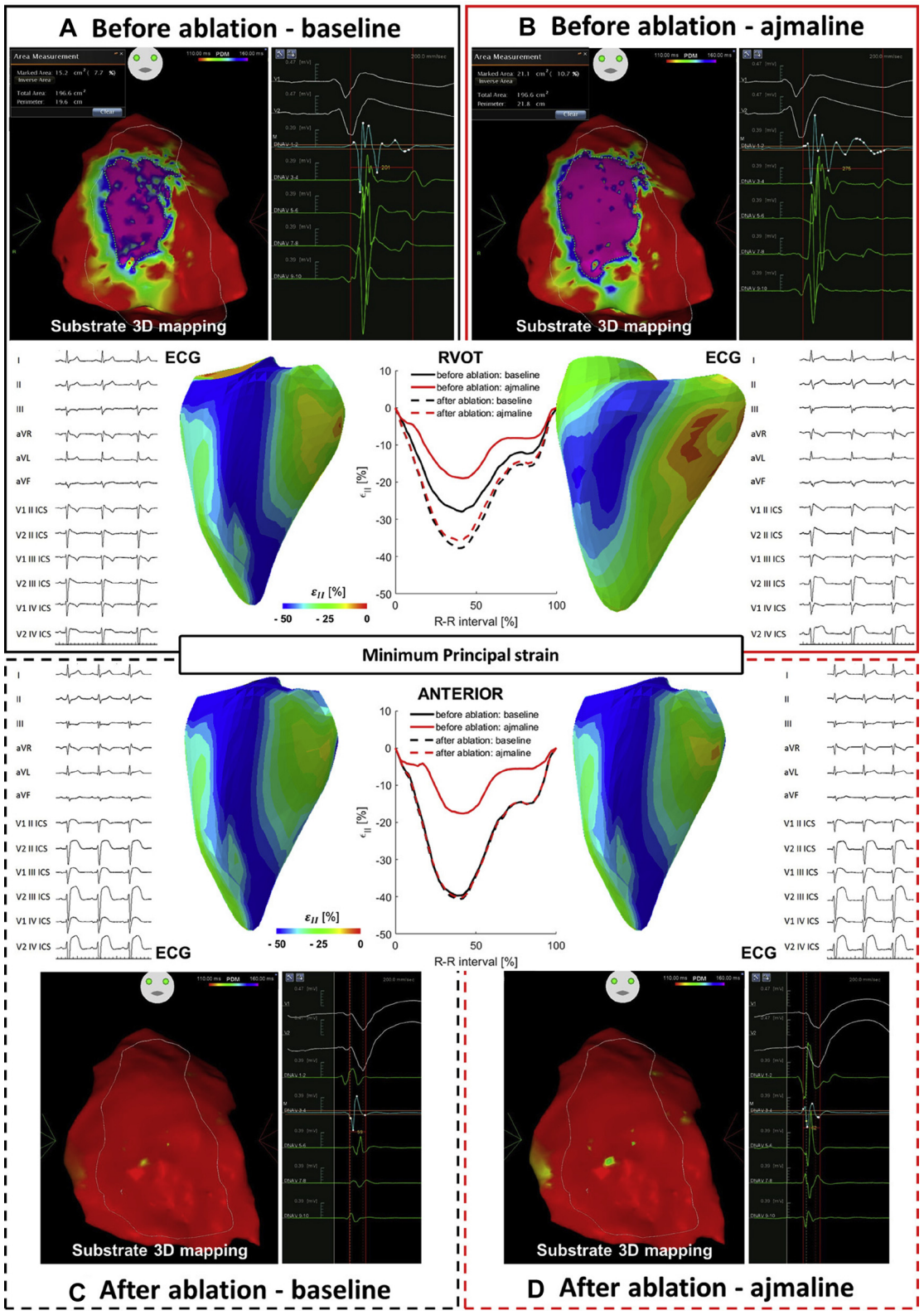

Figure 1 A 46-year-old patient with type 1 electrocardiographic (ECG) pattern. Three-dimensional (3D) substrate mapping and minimum principal strain (ε_{II}) pattern analysis are shown before (**top panels A and B**) and after (**bottom panels C and D**) epicardial ablation. In the **left panel on top**, the baseline potential duration map shows a substrate area (*purple area*), characterized by wide and delayed fragmented potentials (duration $\geq$ 160 ms) located in the right ventricular outflow tract (RVOT)/anterior free wall of the right ventricle (RV). Ajmaline increased the substrate size from 15.2 to 21.1 cm^2 (**upper right panel**) corresponding to a worsening of coved type 1 ST-segment elevation followed by a remarkable impairment of ε_{II} (**middle panel**). Long-duration and fragmented ventricular potentials also increased (from 201 to 275 ms) after ajmaline. The **bottom panels** show postablation 3D electroanatomic maps and the minimum principal strain (ε_{II}) pattern. Substrate ablation normalizes the contractility of the RVOT, and ajmaline rechallenge is no longer able to produce abnormally prolonged electrograms, Brugada-ECG pattern, and reduction in ε_{II} in the RVOT/anterior free wall.

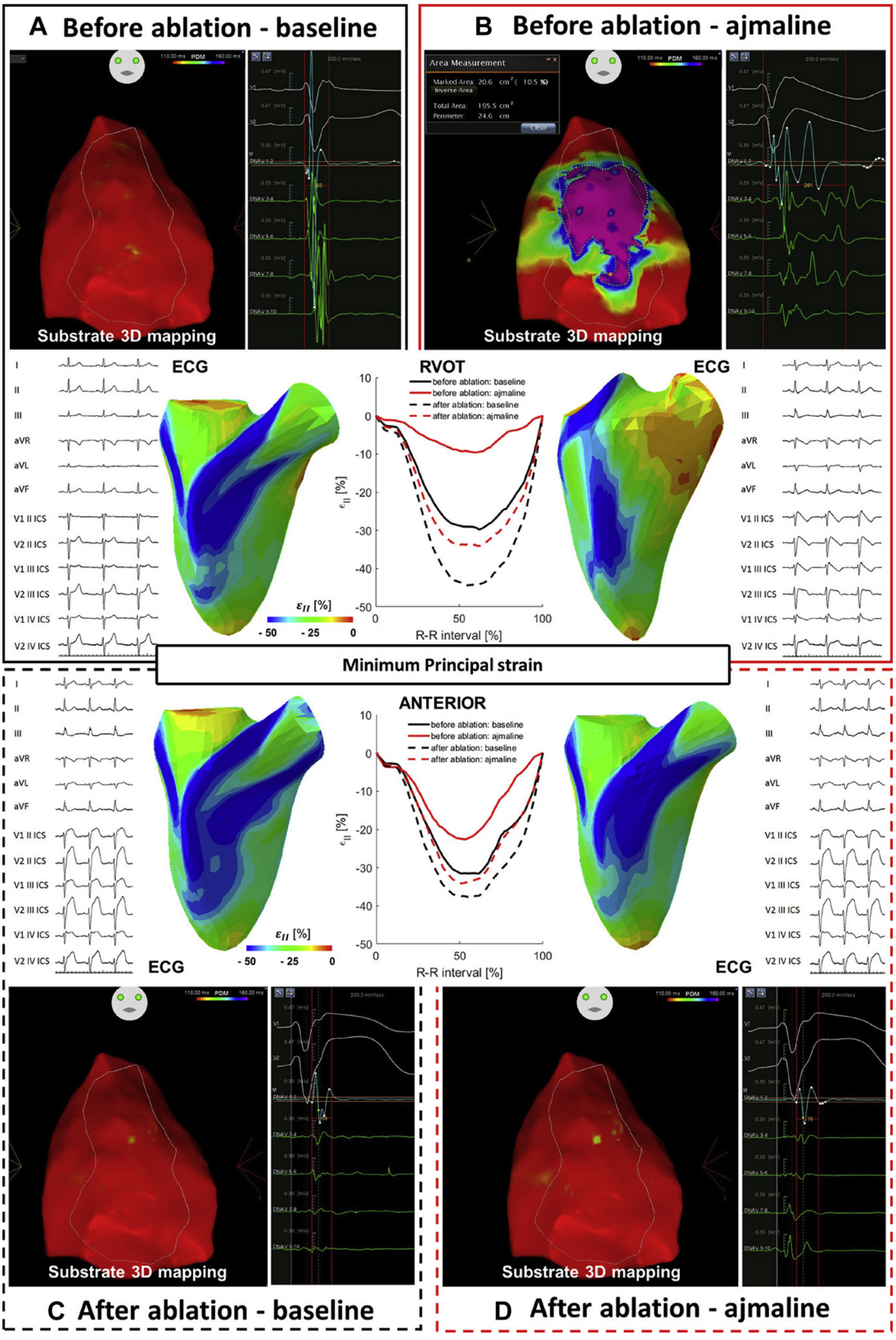

Figure 2 A 45-year-old patient with no type 1 electrocardiographic (ECG) pattern. As in Figure 1, substrate mapping and minimum principal strain (ε_{II}) pattern analysis are shown before (**top panels A and B**) and after (**bottom panels C and D**) ablation. Ajmaline (**right panel on top**) unmasks a concealed substrate area of 20.6 cm^2 (*purple area* in the potential duration map with long duration potentials $\geq$ 160 ms), which is absent at baseline (**left panel on top**) and located in the right ventricular outflow tract (RVOT) epicardium. The substrate is characterized by abnormally prolonged and fragmented potentials, as compared with the baseline value (281 ms vs 69 ms; **upper right panel**). In the same region, a remarkable impairment of ε_{II}, corresponding to the substrate area, is shown in the **middle panel**. The **bottom panels** (**panels C and D**) show that after ablation, ajmaline was no longer able to produce abnormally prolonged electrograms, BrS-ECG pattern on the ECG, or reduction in ε_{II}.

ajmaline ($r = 0.728$, $P < .001$). By multivariate logistic regression analysis, only the extent of the area with RV dysfunction was an independent predictor of VT/VF (odds ratio 1.480; 95% confidence interval 1.159–1.889; $P = .002$).

Postablation echocardiography

In all patients with BrS, during retesting 3 months after the procedure, regardless of their clinical presentation, ajmaline provocation did not induce any ECG abnormalities. The echocardiographic parameters (Table 3) and the area of 3D RV dysfunction also normalized despite ajmaline challenge, reverting to values similar to those of controls (Table 2). The RV motion/deformation parameters did not change after substrate ablation (Supplemental Table 5).

Complications

No patients had major complications resulting from electrophysiology study, mapping, or ablation. No ventricular tachyarrhythmias developed during ajmaline, which was administered at a total dose of 1 mg/kg in 5 minutes. Mild pericarditis pain without hospitalization prolongation occurred in 3 patients. No major groin complications developed that required blood transfusion or surgical intervention.

Discussion

Main findings

Our study confirms and extends the results of prior studies[3–14] reporting the characterization and quantification of electrical and mechanical abnormalities before and after substrate ablation in the presence of a stable type 1 ECG pattern. We also correlated the epicardial map findings with RV mechanical changes after ajmaline. In previous research, the rate of mechanical abnormalities varied greatly across reports, which commonly included patients with BrS with no type 1 ECG pattern, but ajmaline provocation was not systematically administered, as in our study.[8–21] In addition, the relative thinness and complex geometry of the RV, particularly of the RVOT, makes the presence of subtle mechanical abnormalities exceedingly challenging to be assessed using 2D strain parameters alone.

Table 3 Post-RFA echocardiographic parameters before and after ajmaline administration in 50 patients with BrS

Variable	Baseline	Ajmaline	*P*
RV EDV	80.39 ± 14.53	80.44 ± 14.41	.590
RV ESV	35.06 ± 8.13	35.04 ± 8.11	.192
RV Sv	45.36 ± 8.71	45.45 ± 8.66	.170
RV EF 3D	56.51 ± 3.82	56.33 ± 3.85	.247
TAPSE	18.71 ± 3.58	18.67 ± 3.50	.606
FAC	45.39 ± 5.43	45.37 ± 5.42	.269

3D = 3-dimensional; BrS = Brugada syndrome; EDV = end-diastolic volume; EF = ejection fraction; ESV = end-systolic volume; FAC = fractional area change; RFA = RF ablation; RV = right ventricular; Sv = stroke volume; TAPSE = tricuspid annular plane systolic excursion.

Assessing electrical and mechanical abnormalities

In this study, for evaluating RV and LV function we used 3D echocardiography and 3D motion/deformation analysis including spatial distribution and direction, which have been validated through cardiac magnetic resonance,[23–25] because this approach is more reproducible than the 4-chamber view.[26,27] Recently, 3D motion/deformation parameters have been exploited to early detect and objectively quantify subtle regional RV mechanical dysfunction in arrhythmogenic RV cardiomyopathy and pulmonary hypertension,[28,29] but to date, not in patients with BrS. In the present investigational imaging protocol study, we enrolled 50 high-risk patients with BrS with ICD implantation referred for substrate mapping/ablation. Although the majority of patients had ICD implantation for secondary prevention (70%), only a minority (40%) presented with spontaneous type 1 BrS-ECG pattern. Epicardial mapping showed that patients with spontaneous type 1 pattern exhibited larger substrates, which after ajmaline doubled (from 15 to 25.6 cm^2), while the highest absolute increase was observed in the subgroup of patients without spontaneous type 1 pattern (from 2.3 to 17 cm^2). Noteworthy, although patients receiving ICD for primary and secondary prevention showed a similar electrical substrate size, the increase in the substrate after ajmaline was higher in the secondary prevention group. In the presence of ajmaline-induced type 1 BrS pattern, we found different RV areas characterized by consistent heterogeneity of local myocardial mechanics, particularly in the anterior free wall and RVOT, as compared with those of normal controls. These findings indicate that in patients with BrS, electrical and mechanical abnormalities can be the result of a common mechanism. Indeed, as compared with no significant changes in normal controls, in patients with BrS the lower normal displacement after ajmaline revealed significant RV impaired wall motility (from >3 to 0.19 mm after ajmaline), resulting in minimal RV wall inward motion during RV systolic contraction. This finding was paralleled by a substantial worsening of RV wall deformation, particularly in the anterior free wall, with reduction in both areal strain (from −39% to −26%) and minimum principal strain (from −32% to −24%), pinpointing a markedly diminished regional free-wall shortening capacity during RV contraction. As compared with controls and despite similar increases in QRS and QT intervals, such consistent mechanical regional changes occurred only after ajmaline-induced type 1 pattern, which suggests that RV dysfunction was indeed related to electrical substrate expansion and not solely to conduction/electrophysiological abnormalities.

Correlation between electrical and mechanical changes

The most striking and novel finding of our study was the correlation between substrate size and mechanical changes, and this is congruent with previous experimental observations.[30] In our study, electrical substrate expansion and the area of RV dysfunction significantly increased after ajmaline, and

this change lasted concomitantly with the presence of the Brugada type 1 pattern. Interestingly, in multivariate logistic regression analysis, only the extent of the RV dysfunction area was an independent predictor of VT/VF.

Effect of substrate ablation on electromechanical abnormalities

In this study, the finding that substrate ablation not only removed acute electromechanical changes despite ajmaline administration but also abolished the BrS-ECG pattern suggests that a common single mechanism underlies electromechanical abnormalities and BrS-ECG pattern. This observation, however, does not necessarily exclude the presence of structural abnormalities for the BrS substrates, as suggested by recent studies.[15,16] Indeed, if we accept that most structural abnormalities are acquired throughout life, we can understand the rarity of spontaneous type 1 BrS-ECG pattern in children and the relatively late age of diagnosis of BrS.[31] In this context, we can speculate that in BrS, even small electromechanical substrates under specific conditions may become more consistent over time, probably becoming stable over years, and then facilitate structural changes in the RV. The finding that RV dysfunction was no longer inducible by ajmaline rechallenge 3 months after ablation is clinically relevant, but the mechanism remains speculative. One possible explanation may be that in our study, using short RF application times, the total amount of relative voltage reduction was located only in patchy areas of the epicardium and never involving the endocardial layer. In addition, after substrate elimination the mechanical evaluation was performed only 3 months after the procedure, not immediately after ablation. Finally, we believe that the improvement in RV dysfunction after substrate elimination may indicate that not mechanical factor but the specific electrophysiological substrates are the culprit.

Clinical implications

These results are clinically relevant, providing conclusive evidence that type 1 BrS-ECG pattern and mechanical abnormalities are both related to the presence and activation of an extensive RV electrical substrate, as exposed by ajmaline. These findings support the need to perform ajmaline testing and noninvasive 3D echocardiography imaging to potentially reveal and determine concealed abnormal substrates for risk stratification.

Conclusion

BrS is complex RV cardiomyopathy, rather than a purely electrical disease, in which the typical ECG pattern reflects consistent electromechanical substrates in different regions of the RV, particularly in the anterior free wall of the RVOT.

Appendix

Supplementary data

Supplementary data associated with this article can be found in the online version at 10.1016/j.hrthm.2019.11.019.

References

1. Antzelevitch C, Yan GX, Ackerman MJ, et al. J-wave syndromes expert consensus conference report: emerging concepts and gaps in knowledge. Heart Rhythm 2016;13:e295–e324.
2. Sacher F, Probst V, Iesaka Y, et al. Outcome after implantation of a cardioverter-defibrillator in patients with Brugada syndrome: a multicenter study. Circulation 2006;114:2317–2324.
3. Nademanee K, Veerakul G, Chandanamattha P, et al. Prevention of ventricular fibrillation episodes in Brugada syndrome by catheter ablation over the anterior right ventricular outflow tract epicardium. Circulation 2011;123:1270–1279.
4. Brugada J, Pappone C, Berruezo A, et al. Brugada syndrome phenotype elimination by epicardial substrate ablation. Circ Arrhythm Electrophysiol 2015;8:1373–1381.
5. Pappone C, Brugada J, Vicedomini G, et al. Electrical substrate elimination in 135 consecutive patients with Brugada syndrome. Circ Arrhythm Electrophysiol 2017;10:e005053.
6. Pappone C, Ciconte G, Manguso F, et al. Assessing the malignant arrhythmic substrate in patients with Brugada syndrome. J Am Coll Cardiol 2018;71:1631–1646.
7. Coronel R, Casini S, Koopmann TT, et al. Right ventricular fibrosis and conduction delay in a patient with clinical signs of Brugada syndrome: a combined electrophysiological, genetic, histopathologic, and computational study. Circulation 2005;112:2769–2777.
8. Corrado D, Nava A, Buja G, et al. Familial cardiomyopathy underlies syndrome of right bundle branch block, ST segment elevation and sudden death. J Am Coll Cardiol 1996;27:443–448.
9. Takagi M, Aihara N, Kuribayashi S, et al. Localized right ventricular morphological abnormalities detected by electron-beam computed tomography represent arrhythmogenic substrates in patients with the Brugada syndrome. Eur Heart J 2001;22:1032–1041.
10. Papavassiliu T, Wolpert C, Fluchter S. Magnetic resonance imaging findings in patients with Brugada syndrome. J Cardiovasc Electrophysiol 2004;15:1133–1138.
11. Murata K, Ueyama T, Tanaka T, et al. Right ventricular dysfunction in patients with Brugada-like electrocardiography: a two dimensional strain imaging study. Cardiovasc Ultrasound 2011;9:30.
12. Hoogendijk MG, Potse M, Linnenbank AC, et al. Mechanism of right precordial ST-segment elevation in structural heart disease: excitation failure by current-to-load mismatch. Heart Rhythm 2010;7:238–248.
13. Catalano O, Antonaci S, Moro G, et al. Magnetic resonance investigations in Brugada syndrome reveal unexpectedly high rate of structural abnormalities. Eur Heart J 2009;30:2241–2248.
14. Scheirlynck E, Van Malderen S, Motoc A, et al. Contraction alterations in Brugada syndrome; association with life-threatening ventricular arrhythmias. Int J Cardiol 2019;299:147–152.
15. Nademanee K, Raju H, de Noronha SV, et al. Fibrosis, connexin-43, and conduction abnormalities in the Brugada syndrome. J Am Coll Cardiol 2015;66:1976–1986.
16. Pieroni M, Notarstefano P, Oliva A, et al. Electroanatomic and pathologic right ventricular outflow tract abnormalities in patients with Brugada syndrome. J Am Coll Cardiol 2018;72:2747–2757.
17. van Hoorn F, Campian ME, Spijkerboer A, et al. SCN5A mutations in Brugada syndrome are associated with increased cardiac dimensions and reduced contractility. PLoS One 2012;7:e42037.
18. Bastiaenen R, Cox AT, Castelletti S, et al. Late gadolinium enhancement in Brugada syndrome: a marker for subtle underlying cardiomyopathy? Heart Rhythm 2017;14:583–589.
19. Gray B, Gnanappa GK, Bagnall RD, et al. Relations between right ventricular morphology and clinical, electrical and genetic parameters in Brugada syndrome. PLoS One 2018;13:e0195594.
20. Tessa C, Del Meglio J, Ghidini Ottonelli A, et al. Evaluation of Brugada syndrome by cardiac magnetic resonance. Int J Cardiovasc Imaging 2012;28:1961–1970.
21. Papavassiliu T, Veltmann C, Doesch C, et al. Spontaneous type 1 electrocardiographic pattern is associated with cardiovascular magnetic resonance imaging changes in Brugada syndrome. Heart Rhythm 2010;7:1790–1796.
22. Lang RM, Badano LP, Mor-Avi V, et al. Recommendations for cardiac chamber quantification by echocardiography in adult: an update from the American Society of Echocardiography and the European Association of Cardiovascular Imaging. Eur Heart J Cardiovasc Imaging 2015;16:233–270.
23. Satriano A, Heydari B, Narous M, et al. Clinical feasibility and validation of 3D principal strain analysis from cine MRI: comparison to 2D strain by MRI and 3D speckle tracking echocardiography. Int J Cardiovasc Imaging 2017;33:1979–1992.
24. Park JH, Negishi K, Kwon DH, et al. Validation of global longitudinal strain and strain rate as reliable markers of right ventricular dysfunction: comparison with cardiac magnetic resonance and outcome. J Cardiovasc Ultrasound 2014;22:113–120.

25. Muraru D, Spadotto V, Cecchetto A, et al. New speckle-tracking algorithm for right ventricular volume analysis from three-dimensional echocardiographic data sets: validation with cardiac magnetic resonance and comparison with the previous analysis tool. Eur Heart J Cardiovasc Imaging 2016;17:1279–1289.
26. Addetia K, Muraru D, Badano LP, Lang RM. New directions in right ventricular assessment using 3-dimensional echocardiography. JAMA Cardiol 2019; 4:936–944.
27. Genovese D, Mor-Avi V, Palermo C, et al. Comparison between four-chamber and right ventricular-focused views for the quantitative evaluation of right ventricular size and function. J Am Soc Echocardiogr 2019;32:484–494.
28. Mast TP, Teske AJ, Walmsley J, et al. Right ventricular imaging and computer simulation for electromechanical substrate characterization in arrhythmogenic right ventricular cardiomyopathy. J Am Coll Cardiol 2016; 68:2185–2197.
29. Moceri P, Duchateau N, Baudouy D, et al. Three-dimensional right-ventricular regional deformation and survival in pulmonary hypertension. Eur Heart J Cardiovasc Imaging 2018;19:450–458.
30. Dong M, Niklewski PJ, Wang HS. Ionic mechanisms of cellular electrical and mechanical abnormalities in Brugada syndrome. Am J Physiol Heart Circ Physiol 2011;300:H279–H287.
31. Hoogendijk MG, Opthof T, Postema PG, et al. The Brugada ECG pattern: a marker of channelopathy, structural heart disease, or neither? Toward a unifying mechanism of the Brugada syndrome. Circ Arrhyth Electrophysiol 2010; 3:283–290.